Actinonin, a Naturally Occurring Antibacterial Agent, Is a Potent Deformylase Inhibitor

Dawn Z. Chen, Dinesh V. Patel, Corinne J. Hackbarth, Wen Wang, Geoffrey Dreyer, Dennis C. Young, Peter S. Margolis, Charlotte Wu, Zi-Jie Ni, Joaquim Trias, Richard J. White, and Zhengyu Yuan*

Versicor, Inc., 34790 Ardentech Court, Fremont, California 94555

Received September 27, 1999; Revised Manuscript Received December 2, 1999

ABSTRACT: Peptide deformylase (PDF) is essential in prokaryotes and absent in mammalian cells, thus making it an attractive target for the discovery of novel antibiotics. We have identified actinonin, a naturally occurring antibacterial agent, as a potent PDF inhibitor. The dissociation constant for this compound was 0.3×10^{-9} M against Ni−PDF from *Escherichia coli*; the PDF from *Staphylococcus aureus* gave a similar value. Microbiological evaluation revealed that actinonin is a bacteriostatic agent with activity against Gram-positive and fastidious Gram-negative microorganisms. The PDF gene, *def*, was placed under control of P_{BAD} in *E. coli tolC*, permitting regulation of PDF expression levels in the cell by varying the external arabinose concentration. The susceptibility of this strain to actinonin increases with decreased levels of PDF expression, indicating that actinonin inhibits bacterial growth by targeting this enzyme. Actinonin provides an excellent starting point from which to derive a more potent PDF inhibitor that has a broader spectrum of antibacterial activity.

In eubacteria, protein synthesis is initiated with *N*-formylmethionine. In most cases, the newly synthesized polypeptide is converted to mature protein through the sequential removal of the *N*-formyl group and methionine by peptide deformylase and methionine amino peptidase, respectively (Scheme 1; *1*, *2*). In some cases, the formyl group is removed but the initiator methionine is retained.

In *Escherichia coli*, PDF[1] is encoded by the *def* gene, homologues of which are present in all of the bacterial genomes sequenced to date. In those cases that have been studied, the PDF enzymes share many common properties (*3*). PDF activity was first described in 1968 (*1*), but efforts to purify it were hampered due to instability. Subsequent studies have shown that the instability is due to the oxidation of a ferrous ion at the enzyme's active site (*4*).

Although several classes of antibiotics target protein synthesis (e.g., tetracyclines, aminoglycosides, macrolides, and oxazolidinones), there is no report of an antibacterial that inhibits post-translational protein modification. PDF is a potentially attractive target for antibacterial drug design because (a) the gene associated with this activity is essential to bacterial growth in vitro (*5*−*7*), (b) it is present in all eubacteria examined and therefore can lead to broad spectrum activity, (c) the methionine formylation and deformylation cycle is not involved in eukaryotic cytoplasmic protein synthesis, which provides a sound basis for selective toxicity, and (d) the enzyme's active center is very similar to several well-studied metallo hydrolases, including thermolysin and matrilysin, which thus provide prototypes for inhibitor design (*8*−*12*).

Scheme 1: Reaction Catalyzed by PDF and MAP

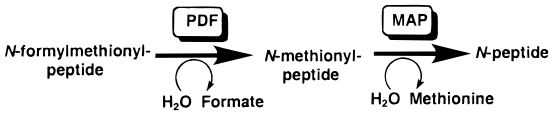

PDF belongs to a new class of metallo hydrolases that utilize an Fe^{2+} ion as the catalytic metal ion (*4*, *13*, *14*). The ferrous ion in PDF is very unstable and can be quickly and irreversibly oxidized into ferric ion, resulting in an inactive enzyme (*15*). Interestingly, the ferrous ion can be replaced with a nickel ion, resulting in little loss of enzyme activity and much greater stability. On the other hand, substitution with zinc results in a more than 10^5-fold loss of activity (*13*). The three-dimensional structures of several forms of PDF have been reported in the literature (*8*−*11*, *16*). The catalytic metal ion of PDF is tetrahedrally coordinated with two histidines from the conserved zinc hydrolase sequence, HEXXH, and a conserved cysteine from an EGCLS motif. The fourth position in the tetrahedron is occupied by a water molecule that presumably hydrolyzes the amide bond.

Several transition state and/or substrate analogue-based inhibitors of PDF have been designed and recently reported (*11*, *17*−*19*). Unfortunately, none of these inhibitors exhibit antibacterial activity, presumably due to a lack of potency against PDF and/or an inability to penetrate the bacterial cell. In this study, we report that actinonin, a naturally occurring antibacterial agent (*20*), is a very potent reversible PDF inhibitor and present evidence that actinonin inhibits bacterial growth through the inhibition of PDF activity.

* To whom correspondence should be addressed. Phone: (510) 739-3026. Fax: (510) 739-3003. E-mail: zyuan@versicor.com.

[1] Abbreviations: PDF, peptide deformylase; MAP, methionine amino peptidase; fMAS, *N*-formylmethionine-alanine-serine; FDH, formate dehydrogenase; NAD^+, nicotinamide adenine dinucleotide; NADH, nicotinamide adenine dinucleotide, reduced form; IPTG, isopropyl thiogalactopyranoside; LB medium, Luria-Bertani medium; TSB, tryptic soy broth; PDB, Protein Data Bank.

10.1021/bi992245y CCC: $19.00
Published on Web 01/19/2000

MATERIALS AND METHODS

Materials. Actinonin, formate dehydrogenase, catalase, and NAD^+ were obtained from Sigma; *N*-formylmethionine-alanine-serine was obtained from Bachem. All other chemicals were of the highest commercial grade.

Overexpression of PDF from E. coli and Staphylococcus aureus. The *E. coli def* gene and *S. aureus defB* gene were PCR amplified from genomic DNA of *E. coli* JM109 and *S. aureus* NCTC8325-4, respectively, and cloned into expression vector pET20b$^+$ (Novagen). The *def* gene-containing constructs were confirmed by DNA sequence analysis and used to transform *E. coli* BL21(DE3) pLysS. *E. coli* containing the expression vector was grown at 30 °C in LB medium to a density where $OD_{600} = 0.5$ and then induced with 100 μM IPTG for 5 h before harvesting by centrifugation. The cells from 1 L of culture medium were resuspended into 70 mL of buffer containing 20 mM Tris (pH 8.0) and 10 mM NaCl.

Enzyme Purification. For preparation of the "Fe−PDF" enzyme, the cells containing overexpressed PDF were lysed in the presence of 10 μg/mL catalase by passing them through a French press. The presence of catalase can prevent the oxidation of ferrous ion and stabilize the native ferrous form of PDF (*13*). This cell lysate had very high enzyme activity; a protein of the expected size was the major band on SDS−PAGE. Further steps of purifying Fe−PDF from this lysate resulted in a cleaner protein, albeit with a lower specific activity, which was probably due to the oxidation of the ferrous ion. Therefore, these Fe−PDF-containing cell lysates were used directly without further purification. After the background had been subtracted, the enzyme activity in this lysate was very specific and could be completely inhibited by PDF inhibitors. PDFs in which the ferrous ion was replaced with nickel ion in their active center (Ni−PDF) were prepared by the ion exchanging protocol of Groche et al. (*13*). To replace the ferrous ion, 5 mM $NiCl_2$ was added to the cell suspension before it was passed through a French press. The resulting Ni−PDF was purified on a HiLoad 16/10 Q-Sepharose ion exchange column (Pharmacia) in the presence of 5 mM $NiCl_2$. Using a linear elution gradient of KCl, *E. coli* and *S. aureus* Ni−PDFs eluted at 220 and 140 mM, respectively. The "Zn−PDF" was expressed in *E. coli* as a C-terminal His_6-tagged protein in the pET20b$^+$ expression vector. Purification of the overexpressed His_6-tagged PDF was carried out on a Co^{2+} affinity column (Clontech) without catalase present, which resulted mainly in the Zn form of PDF (*4*, *21*). However, this enzyme preparation may also contain PDF with other metal ions in the active center (*13*). The enzyme concentration was determined using the Bio-Rad Protein Assay Kit (Bio-Rad) with BSA as the standard. Specific activities obtained for these PDFs were similar to those reported in the literature (*4*, *13*, *21*).

Enzyme Assay. The PDF/FDH coupled assay (*22*) was used for all enzymatic activity measurements. In this coupled assay, the formate released by PDF from its substrate fMAS is oxidized by the coupling enzyme FDH, reducing one molecule of NAD^+ to NADH, which causes an increase in absorption at 340 nm. In this study, all assays were carried out at room temperature in a buffer of 50 mM HEPES (pH 7.2), 10 mM NaCl, and 0.2 mg/mL BSA, in half-area 96-well microtiter plates (Corning). The reaction was initiated by adding a mixture of 0.5 unit/mL FDH, 1 mM NAD^+, and fMAS at the desired concentration. To determine IC_{50} (the concentration needed to inhibit 50% of enzyme activity) values, PDF was preincubated for 10 min with varying concentrations of actinonin, and the deformylation reaction was initiated by the addition of a reaction mixture containing 4 mM fMAS. The initial reaction velocity, *y*, was measured as the initial rate of absorption increase at 340 nm using a SpectraMax plate reader (Molecular Devices). The inhibitor concentration which can inhibit 50% of enzyme activity, IC_{50}, was calculated using eq 1:

$$y = y_o/(1 + IC_{50}/[In]) \quad (1)$$

To determine the dissociation constant for dissociation of actinonin from PDF, initial reaction velocities were measured with varying concentrations of fMAS at several actinonin concentrations. The data were then calculated according to the method of Henderson, which can be used to determine the dissociation constant of tight binding competitive enzyme inhibitor (*23*):

$$[In]/(1 - v_i/v_o) = [En] + K_i(v_o/v_i)(1 + [S]/K_m) \quad (2)$$

where [In], [En], and [S] are the total concentrations of inhibitor, enzyme, and substrate, respectively, v_i and v_o are reaction rates in the presence and absence of inhibitor, respectively, and K_m is the Michaelis constant for the substrate fMAS.

All data fitting was carried out with nonlinear least-squares regression using the commercial software package DeltaGraph 4.0 (Deltapoint, Inc.).

Modeling of Actinonin Binding. A model of actinonin bound to PDF was constructed using two sets of crystallographic coordinates as templates: uncomplexed Zn−PDF [Protein Data Bank (PDB) entry 1dff; *10*] and matrilysin complexed to a hydroxamate-based inhibitor (PDB entry 1mmq; *12*). Conformational energy minimization was carried out with MacroModel version 5.5 (*24*), while initial manual docking and visualization of final results were performed with MidasPlus version 2.0 (*25*). The 1mmq and 1dff coordinates were aligned by least-squares fitting backbone atoms of residues 218−222 (1mmq) to residues 132−136 (1dff), and then torsion angles of actinonin were adjusted to a conformation resembling that of the 1mmq hydroxamate inhibitor and consistent with the 1dff solvent-accessible molecular surface. To refine the actinonin−PDF model, the Zn atom was removed (to overcome limits in force field parametrization) and the inhibitor conformation was minimized within the rigid protein (applying a 15 Å restraining shell of 400 kJ/Å around the inhibitor) using the AMBER force field with water solvation as implemented in MacroModel (*24*−*26*).

Susceptibility Tests. (1) Minimum Inhibitory Concentration (MIC). MICs were determined against ATCC strains recommended for antibiotic susceptibility testing (*27*). *Enterococcus faecium* strains BM4147.1 and BM4147 (a vancomycin-resistant strain derived from BM4147.1) were gifts from P. Courvalin (Institute Pasteur, Paris, France). The *E. coli acr* and *Haemophilus influenzae acr* strains are efflux pump mutants, which were gifts from H. Nikaido (University of California, Berkeley, CA). Microdilution MICs were deter-

mined in 96-well microtiter plates in Mueller-Hinton broth (Becton Dickinson) following the guidelines of the National Committee for Clinical Laboratory Standards (*27*) but with a starting inoculum of 1×10^5 cfu/mL. The MIC was the lowest concentration of drug that yielded no visible growth after incubation for 18−24 h at 35 °C.

(2) Time Kill Experiments. S. aureus strain ATCC 25923 was exposed to actinonin or vancomycin (Sigma) at 10 × MIC in TSB. Flasks containing 5×10^5 cfu/mL of log phase organisms were placed in a shaking 37 °C incubator, and viable counts were quantitatively determined after incubation for 0, 2, 6, and 24 h. Results were plotted as log(cfu/mL) over time.

P_{BAD}-def-Regulated E. coli Strain. Using a promoter exchange strategy, the *def* gene was placed under arabinose control in a *tolC*-deficient *E. coli* strain. Promoter exchange vectors contain two regions of chromosomal homology which flank a 1.3 kb kanamycin resistance cassette and a 1.6 kb arabinose regulatory region. One region of chromosomal homology is the full-length essential gene; the second region of homology is 600 bp of DNA corresponding to a chromosomal sequence immediately upstream of the essential gene. The vector is used to replace the endogenous promoter of an essential gene with the P_{BAD} promoter using conventional allele replacement techniques (*28*, *29*). With this construct, PDF expression in *E. coli* can be up- or downregulated by varying arabinose concentrations in the growth medium. When PDF is downregulated, the resulting bacteria should be much more sensitive to PDF inhibitors. Checkerboard assays were performed to determine the association between the susceptibility of potential PDF inhibitors and arabinose concentration. Bacteria were grown overnight at 35 °C in LB supplemented with 0.2% arabinose. The cell suspension was washed several times with LB, diluted 1:1000, and used as inoculum.

RESULTS

Since peptide deformylase is a metallo hydrolase, compounds containing a metal ion chelating group are potential inhibitors of the enzyme. Rather than screen empirically for inhibitors of PDF, we have employed a strategy relying on the fact that the target is a metallo enzyme. Thus, a chemical library collection of more than 25 000 "drug-like" low-molecular weight compounds, about 20% of which contained a metal ion chelating group, was screened in the peptide deformylase assay. The compounds were tested in duplicate at a single concentration in the range of 10−50 μM, and compounds which inhibited more than 50% enzyme activity were defined as hits for further evaluation. As a result of this focused screening, four library members, containing different chelating groups such as hydroxamate, were identified as hits with IC_{50} values of less than 10^{-5} M. On the basis of the structure−activity relationship analysis of these hits, it was recognized that compounds with a methionine-like structure at the P_1' site, together with a chelating group at its N-terminus, might be potential PDF inhibitors. These analyses lead us to hypothesize that actinonin, a naturally occurring antibacterial agent (*20*) that possesses a hydroxamate metal chelating group and a methionine-like structure at the P_1' site, may be exhibiting its antibacterial activity through inhibition of PDF. Subsequent tests confirmed that

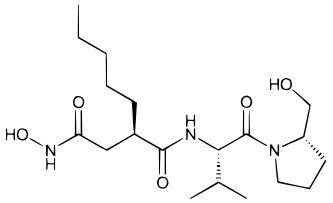

FIGURE 1: Structure of actinonin.

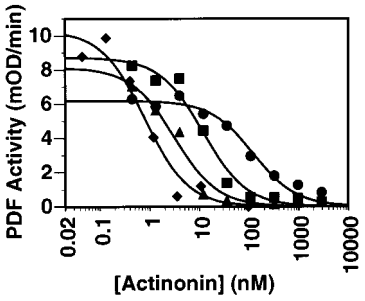

FIGURE 2: Dose−response relationship of actinonin inhibition against various PDFs. Deformylation activities of 770 nM *E. coli* Zn−PDF (●), 6 nM *E. coli* Ni−PDF (▲), *E. coli* Fe−PDF (◆), and 20 nM *S. aureus* Ni−PDF (■) were measured in the presence of 4 mM fMAS and increasing concentrations of actinonin. The curves are the best fit of the data to eq 1 with IC_{50} values of 90, 3, 0.8, and 11 nM for these four forms of PDF, respectively.

actinonin is indeed a very potent PDF inhibitor. Actinonin was first identified in 1962 as an antibiotic produced by an actinomycete and was shown to be active against a number of bacterial species (*20*). The structure of the compound has been determined (*30*) and is shown in Figure 1. Subsequent studies on analogues indicated that the hydroxamate moiety of the molecule is critical for antibacterial activity, but the pseudopeptide backbone can be changed. The mechanism of its antibacterial activity was initially thought to be associated with RNA synthesis, but the evidence supporting this conclusion was not convincing (*31*). In addition to antibacterial activity, actinonin was also reported to inhibit several amino peptidases, such as human seminal alanyl aminopeptidase (*32*), as well as tumor growth (*33*).

Figure 2 depicts the dose-dependent inhibition of various preparations of deformylase by actinonin. As demonstrated in the figure, actinonin is a potent inhibitor of all three forms (Zn−, Ni−, and Fe−) of peptide deformylases from both *S. aureus* and *E. coli* bacteria. Under the assay conditions, the IC_{50} values for actinonin were 90, 3, 0.8, and 11 nM for Zn−PDF (*E. coli*), Ni−PDF (*E. coli*), Fe−PDF (*E. coli*), and Ni−PDF (*S. aureus*), respectively. In a separate control experiment under the same assay conditions, actinonin did not inhibit FDH activity at concentrations up to 10 μM. In comparison, IC_{50} values for all previously reported PDF inhibitors are in the range of 1−10 μM (*11*, *17*−*19*).

The IC_{50} values depicted in Figure 2 for Ni−PDFs are approaching half of the enzyme concentration used in the assay. This suggests that the binding between actinonin and PDF is very tight and that the free inhibitor concentration in the mixture can no longer be approximated by the total inhibitor concentration. Indeed, when the total enzyme concentration was changed, the corresponding IC_{50} also changed (data not shown). Therefore, conventional steady-state kinetics (such as a Lineweaver−Burk plot) cannot be

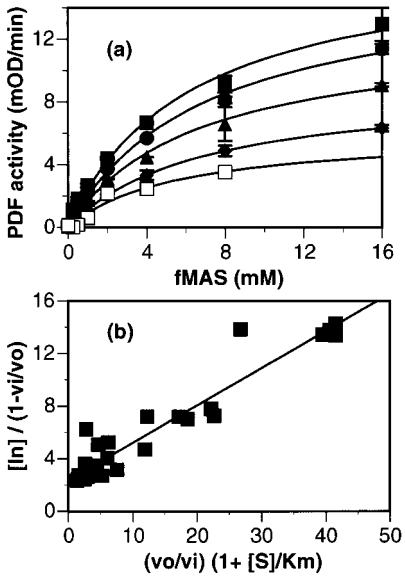

FIGURE 3: Actinonin is a tight binding inhibitor of *E. coli* Ni−PDF with a K_i of 0.3 nM. (a) The enzymatic activity of 6 nM Ni−PDF was plotted with increasing concentrations of substrate fMAS in the presence of 0 (■), 0.4 (●), 0.8 (▲), 1.6 (◆), and 3.25 nM actinonin (□). The error bars are the standard deviation of duplicated data. The curves are the best fit of the data at a fixed actinonin concentration to the Michaelis−Menten equation. For actinonin concentrations of 0, 0.4, 0.8, 1.6, and 3.3 nM, the best-fit parameters are 6.0, 6.9, 6.5, 6.8, and 5.5 mM for the apparent K_m and 17.4, 15.9, 12.4, 9.0, and 6.0 mOD/min for the apparent V_{max}, respectively. (b) Data depicted in panel a were reanalyzed according to eq 2 and plotted as indicated. The line represents the linear least-squares fit of the data. On the basis of this method, the dissociation constant for actinonin against *E. coli* Ni−PDF is 0.28 nM with a total free enzyme concentration of 2.4 nM.

applied to determine the dissociation constant (K_i). To determine the true dissociation constant for dissociation of *E. coli* Ni−PDF from actinonin, reaction rates versus substrate concentrations were measured in the presence of several different concentrations of actinonin (Figure 3a) and an enzyme concentration of 6 nM (calculated on the basis of the Bio-Rad protein concentration assay). The curves in Figure 3a are the best fit of the data, at a constant actinonin concentration, to the Michaelis−Menten equation. These data were further manipulated according to eq 2, and plotted as $[In]/(1 - v_i/v_o)$ versus $(v_o/v_i)(1 + [S]/K_m)$, as shown in Figure 3b. In this plot, 6 mM was used as the K_m value, which is the Michaelis constant measured in the absence of inhibitor. The best fit of these data to eq 2 gives a dissociation constant of 0.28 nM and a total enzyme concentration of 2.4 nM. The total enzyme concentration derived here is about one-half of that determined with the Bio-Rad protein assay kit, which is consistent with a previous finding that the PDF concentration is 56% of the value determined with the same commercial kit (*21*). Alternatively, this may simply reflect the fraction of active enzyme in the protein preparation.

To further understand the inhibition of PDF by actinonin, the reaction was initiated by the addition of *E. coli* Zn−PDF, and reaction progress was followed by measuring the absorption increase at 340 nm. The slope of the reaction progress curve did not decrease over the initial 15 min of the reaction. In addition, the IC_{50} values for actinonin remained unchanged with the preincubation time ranging from 10 to 100 min. These data suggest that the binding of actinonin to Zn−PDF is fast and that there is no slow-binding process occurring between PDF and actinonin. The reversibility of actinonin inhibition of PDF also was examined. Mixtures containing 1 μM Zn−PDF with and without 1.5 μM actinonin were prepared at room temperature, and there was no detectable deformylase activity under these conditions. These samples were then subjected to extensive dialysis at 4 °C against several changes of a buffer containing 50 mM HEPES (pH 7.2) and 10 mM NaCl. After dialysis for 48 h, PDF activity was measured for both samples. The activity from the enzyme/actinonin mixture (90.8% of that of the original enzyme sample) was very similar to the activity detected from the control sample (90.0% of that of the original enzyme sample). Since the enzyme activity of the actinonin-inhibited PDF was almost completely recovered after removing free actinonin, it was concluded that the inhibition of PDF by actinonin is reversible.

Table 1: MIC Values[a] of Actinonin against Selected Bacteria

bacteria (no. of strains tested)	MIC range (μg/mL)
S. aureus (4)	8−16
Staphylococcus epidermidis (2)	2−4
E. faecium (2)	32−64
Enterococcus faecalis (1)	>64
S. pneumoniae (1)	8
Streptococcus pyogenes (1)	8
E. coli acr (1)	0.25
E. coli (1)	>64
H. influenzae (3)	1−2
H. influenzae acr (1)	0.13
M. catarrhalis (1)	0.5
N. gonorrhoeae (3)	1−4
Bacteroides fragilis (1)	0.25

[a] MICs were determined according to standard methods with a starting inoculum of 1×10^5 cfu/mL. The MIC is expressed as a range for the number of strains that were tested.

Table 1 summarizes the MIC values of actinonin against various bacterial species. Actinonin was active against Gram-positive bacteria, including *S. aureus* and *Streptococcus pneumoniae*. It was also active against fastidious Gram-negative bacteria, such as *H. influenzae*, *Moraxella catarrhalis*, and *Neisseria gonorrheae.* The compound was very active against the *H. influenzae acr* and *E. coli acr* efflux pump mutants; however, it was inactive against wild-type *E. coli*. This spectrum of activity suggests that actinonin can penetrate the bacterial wall and membrane, but is rapidly exported by organisms with an efficient efflux system.

In a 24 h time-kill experiment, there was a slight decrease (<1 log unit) in viable counts when *S. aureus* was exposed to actinonin (80 μg/mL, 10 × MIC), whereas with the bactericidal vancomycin (10 μg/mL, 10 × MIC), the number of organisms decreased more than 3 log units from the initial inoculum. These results suggest that actinonin, like most antibiotics that target protein synthesis, is a bacteriostatic agent.

Although actinonin inhibits bacterial growth and is a potent deformylase inhibitor, it is important to establish that its antibacterial activity results from the inhibition of deformylase. To confirm this hypothesis, the P_{BAD}-*def* construct in *E. coli tolC* was used to assess the compound's mechanism of action in *E. coli*. Because P_{BAD} is a titratable regulated promoter, the level of expression of deformylase in the P_{BAD}-*def* strains will be dependent on, and proportional to, the

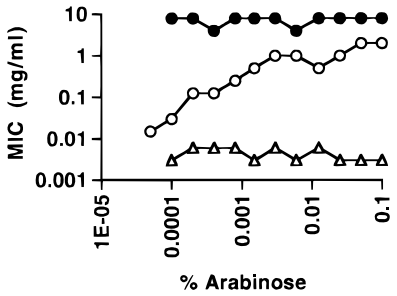

FIGURE 4: Actinonin inhibits bacterial growth through the inhibition of deformylase. The PDF level in the construct P_{BAD}-*def E. coli* is regulated by arabinose concentration. For this construct, the MIC values of actinonin (○), together with control compounds fosfomycin (●) and ciprofloxacin (△), were measured in the presence of increasing concentrations of arabinose. Only actinonin exhibited an association between susceptibility and arabinose concentration.

concentration of inducer (arabinose) in the medium. In a control construct, a reporter gene (*phoA*) was placed under P_{BAD} control on the chromosome; its expression level was shown to be closely correlated with arabinose concentration (*34*). At sufficiently low arabinose concentrations, the target gene *def* will be underexpressed; the cells are expected to become hypersusceptible to PDF-specific inhibitors, but not to inhibitors which act through other mechanisms. Furthermore, an increase in MIC is expected as the arabinose concentration increases. Using checkerboard assays, the susceptibility to actinonin, fosfomycin, and ciprofloxacin was determined, in *E. coli* P_{BAD}-*def tolC*, over a range of arabinose levels. Only actinonin exhibited an association between MIC and the concentration of inducer in the medium (Figure 4). The MIC value was as low as 0.0156 μg/mL at an arabinose concentration of 0.0005%, the lowest at which bacteria could still grow. At the highest arabinose concentration (0.05%), the corresponding MIC was greater than 2 μg/mL, a more than 100-fold increase (Figure 4). As a comparison, the MIC to actinonin for the parent *E. coli tolC* is 0.25 μg/mL. By contrast, the P_{BAD}-*def* strain did not exhibit altered susceptibility to other antibiotics, such as fosfomycin and ciprofloxacin, when the inducer concentration was varied. A second P_{BAD}-*def* strain was constructed using a modified procedure in which the *def* gene was removed from the *def-fmt* operon and placed elsewhere in the chromosome under P_{BAD} control. In this construct, the expression of *fmt* is not affected by changes in the arabinose concentration since *fmt* is still under the control of the original promoter. These two P_{BAD}-*def* strains had nearly identical actinonin susceptibilty profiles under varying arabinose concentrations (*34*). These experiments clearly indicate that actinonin inhibits bacterial growth by inhibition of deformylase, the intended target of this study.

DISCUSSION

In the past decade, there has been a dramatic increase in the number of reports of pathogenic bacteria that are resistant to currently available antibacterials. This is partially due to the fact that all the available antibacterials belong to a limited number of chemical classes, which target a similarly limited number of molecular targets of the bacteria. To develop new antibacterial drugs that work by inhibiting novel targets, many new technologies are being used and several criteria for selecting new targets have been proposed (*35*). Bacterial peptide deformylase appears to satisfy several of these criteria: it is essential to bacterial growth and has no mammalian counterpart. Since there are no clinically used antibacterial agents that target PDF, bacteria already resistant to existing antibiotics should remain susceptible to PDF inhibitors. PDF also is a very attractive target for medicinal chemistry since it belongs to the family of metallo hydrolases, one of the best studied enzyme classes, and there is a rich literature on how to search for and design inhibitors of enzymes of this type.

Actinonin is a tight-binding inhibitor of PDF with a K_i value of 0.28 nM. Under the assay conditions, the IC_{50} for the compound against Ni−PDF was close to one-half of the enzyme concentration. The method of Henderson (*23*) was applied to obtain the dissociation constant for this tight-binding inhibitor. The data best fit a competitive kinetic model with an R^2 of 0.91. As a comparison, fitting the same data to noncompetitive and uncompetitive models yields a much large error ($R^2 = 0.73$ and $R^2 = 0.36$, respectively).

In an effort to understand the structural basis for tight-binding inhibition, we constructed a model of PDF-bound actinonin (Figure 5) by making use of the structural homology between PDF and the zinc protease matrilysin. An overlay of the coordinates of PDF (PDB entry 1dff; *10*) and matrilysin (PDB entry 1mmq; *12*) complexed to a hydroxamate inhibitor, which is similar to actinonin, positions the matrilysin inhibitor in the PDF active site in a manner that plausibly accommodates both polar and hydrophobic contacts; this provided a template for constructing the actinonin model, as described in Materials and Methods.

From the actinonin model and by analogy with previous inhibitors (*11*, *19*), the *n*-pentyl chain defines the probable P_1' site of the inhibitor and functions as an analogue of methionine, the preferred amino acid at P_1' in PDF substrates (*36*). Previous study indicates that an *n*-pentyl group can replace methionine at the P_1' site of the PDF substrate (*37*). The *n*-pentyl chain is well-accommodated but may be slightly long for the S_1' pocket of the enzyme, resulting in an eclipsing interaction at its terminus. As shown in Figure 5, several potential actinonin−PDF hydrogen bonds are pre-

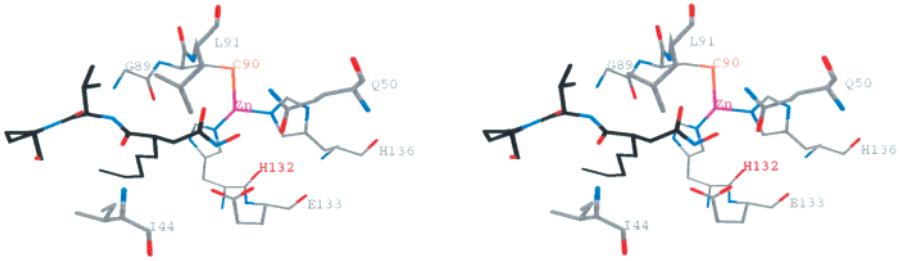

FIGURE 5: Stereoview of the PDF-bound actinonin model. The active metal center of PDF is shown along with surrounding protein residues (gray carbons) that could make polar contacts with actinonin.

dicted by the model, including O(Val)−N(Gly89), N(Val)−O(Gly89), and O(S_1')−N(Ile44). The hydroxamate group is positioned favorably to chelate the active site zinc, and several close polar contacts between the hydroxamate and enzyme side chains may also contribute to the observed tight binding, including CO(hydroxamate)−N(Leu91), N(hydroxamate)−OE2(Glu133), and O(hydroxamate)−NE2(Gln50). Although the conformation of the model in Figure 5 is imprecise due to simplifying assumptions (notably, omission of Zn during minimization), comparison with the structure of PDF complexed with its enzymatic product MetAlaSer (PDB entry 1bs8; *16*) shows good overall agreement in the β-strand-like conformation, the active site placement of side chains, and the direction of H-bond donor and acceptor groups (not shown). Detailed results and the modeling procedure are available from at Versicor's web site (www.versicor.com).

Actinonin is a known hydroxamate-containing inhibitor of several metallo hydrolases. The hydroxamate-containing compounds are very potent inhibitors of metallo enzymes, especially matrix metalloproteases (MMPs) (*38*−*40*). Although several different chelating groups have been reported in the literature, hydroxamate remains the preferred group, and most of MMP inhibitors currently in clinical trials are hydroxamate-based compounds (*40*). The hydroxamate group of actinonin evidently acts as the chelating group to bind the metal ion of the enzyme. Other PDF inhibitors containing similar P_1' groups but with other metal ion binding groups have been reported (*11*, *17*−*19*). These inhibitors all favor a norleucine- or methionine-like four-carbon side chain at P_1', while sporting various P_2' and P_3' substituents. However, the compounds with other metal binding groups are much weaker inhibitors of PDF, with K_i values of 37 μM for phosphonate (*17*), 2.5 μM for sulfhydroxyl (*18*), and 26 and 9.5 μM for aldehyde against Zn− and Co−PDF, respectively (*19*). Previously, the hydroxamate group of actinonin was shown to be essential for maintaining the antibacterial activity (*41*). In addition, modifications of the proline group at P_3' could be made without loss of their activity, provided that the pseudopeptide backbone is retained. Indeed, we have determined that [4-(*N*-hydroxyamino)-2(*R*)-isobutylsuccinyl]-L-*tert*-butylglycine *N*-methylamide, a hydroxamate-containing pseudopeptide without proline at the P_3' site (*42*), is still a potent PDF inhibitor with an IC_{50} of 5 nM (against *E. coli* Ni−PDF). Taken together, these data suggest that the hydroxamate, and not proline at the P_3' site, is primarily responsible for the potent PDF inhibitory activity of actinonin. It is not clear why hydroxamate is the preferred metal-binding group, but polar interactions between the hydroxamate and enzyme residues in the vicinity of the metal binding site could contribute to the high affinity. On the basis of all the experimental results and molecular modeling, we conclude that actinonin is a reversible, competitive, tight-binding PDF inhibitor acting via unusually effective metal chelation.

In this study, actinonin was identified as a potent PDF inhibitor with a K_i of 0.28 nM. Actinonin is also a naturally occurring antibacterial agent which is active against Gram-positive bacteria and fastidious Gram-negative bacteria. Since actinonin has such a high affinity for deformylase, it is logical to suspect that the antibacterial activity of this compound is mainly due to its ability to inhibit PDF, which would result in the accumulation of newly synthesized formyl-methionine-capped inactive peptides and the subsequent cessation of bacterial growth. We have used a novel method to verify the intracellular mechanism of the antibacterial effect of a PDF inhibitor that involves downregulating the amount of target that is expressed. This was achieved through allelic replacement, placing the chromosomal copy of *def* under control of the tightly regulated arabinose promoter, and then testing the impact of inducer (arabinose) concentration on the susceptibility to the inhibitor. The results clearly demonstrated that lowering the arabinose concentration in the growth medium increased the susceptibility of the bacteria. This is presumably mirrored by a decrease in the intracellular levels of PDF and supports the proposal that growth inhibition is achieved through inhibition of this enzyme. Previous experiments aimed at verifying the intracellular mechanism of enzyme inhibitors have employed the overexpression of a putative target enzyme, which can result in increased resistance to the inhibitor. Typically, this has been carried out by putting a second copy of the gene in question on a multicopy plasmid. While this method works well for overexpressing a target enzyme, it does not permit underexpression. Our approach allows one to increase or decrease the level of a target. Furthermore, overexpression alone can be misleading since an enzyme may not be the growth-limiting target but, in excess, it may bind and reduce the concentration of free antibiotic inside the cell, provoking apparently selective resistance. Detailed discussion of this novel approach will be published elsewhere (*34*).

In summary, we have identified actinonin as a potent PDF inhibitor and shown that the antibacterial effect of this compound is due to its inhibition of deformylase activity. In view of its enzymatic profile, antibacterial potency, and structural resemblance to substrates, actinonin can serve as an excellent starting point for rational design of new antibacterial agents that are PDF inhibitors. A complete study of the structure−activity relationships of actinonin analogues and other PDF inhibitors will be published elsewhere.

REFERENCES

1. Adams, J. M. (1968) *J. Mol. Biol. 33*, 571−589.
2. Sherman, F., Stewart, J. W., and Tsunasawa, S. (1985) *BioEssays 3*, 27−31.
3. Meinnel, T., Lazennec, C., Villoing, S., and Blanquet, S. (1997) *J. Mol. Biol. 267*, 749−761.
4. Rajagopalan, P. T. R., Yu, X. C., and Pei, D. (1997) *J. Am. Chem. Soc. 119*, 12418−12419.
5. Mazel, D., Pochet, S., and Marliere, P. (1994) *EMBO J. 13*, 914−923.
6. Chang, S. P., McGary, E. C., and Chang, S. (1989) *J. Bacteriol. 171* (7), 4071−4072.
7. Margolis, P. S., Hackbarth, C. J., Young, D., Wang, W., Chen, D., Yuan, Z., White, R., and Trias, J. (1999) *Antimicrob. Agents Chemother.* (submitted for publication).
8. Meinnel, T., Blanquet, S., and Dardel, F. (1996) *J. Mol. Biol. 262*, 375−386.
9. Dardel, F., Ragusa, S., Lazennec, C., Blanquet, S., and Meinnel, T. (1998) *J. Mol. Biol. 280*, 501−513.
10. Chan, M. K., Gong, W. M., Rajagopalan, P. T. T., Hao, B., Tsai, C. M., and Pei, D. (1997) *Biochemistry 36*, 13904−13909.
11. Hao, B., Gong, W., Rajagopalan, P. T. R., Zhou, Y., Pei, D., and Chan, M. K. (1999) *Biochemistry 38*, 4712−4719.
12. Browner, M. F., Smith, W. W., and Castelhano, A. L. (1995) *Biochemistry 34*, 6602.

13. Groche, D., Becker, A., Schlichting, E., Kabasch, W., Schultz, S., and Wagner, A. F. V. (1998) *Biochem. Biophys. Res. Commun. 246*, 342−346.
14. Ragusa, S., Blanquet, S., and Meinnel, T. (1998) *J. Mol. Biol. 280*, 515−523.
15. Rajagopalan, P. T. R., and Pei, D. (1998) *J. Biol. Chem. 273*, 22305−22310.
16. Becker, A., Schlichting, I., Kabsch, W., Groche, D., Schultz, S., and Wagner, A. F. W. (1998) *Nat. Struct. Biol. 5*, 1053−1058.
17. Hu, Y., Rajagopalan, P. T. R., and Pei, D. (1998) *Bioorg. Med. Chem. Lett. 8*, 2479−2482.
18. Meinnel, T., Patiny, L., Ragusa, S., and Blanquet, S. (1999) *Biochemistry 38*, 4287−4295.
19. Durand, D. J., Green, B. G., O'Connell, J. F., and Grant, S. K. (1999) *Arch. Biochem. Biophys. 367*, 297−302.
20. Gordon, J. J., Kelly, B. K., and Miller, G. A. (1962) *Nature 195*, 701−702.
21. Rajagopalan, P. T. R., Datta, A., and Pei, D. (1997) *Biochemistry 36*, 13910−13918.
22. Lazennec, C., and Meinnel, T. (1997) *Anal. Biochem. 244*, 180−182.
23. Henderson, P. J. F. (1972) *Biochem. J. 127*, 321−333.
24. *MacroModel Interactive Molecular Modeling System*, version 5.5 (1996) Department of Chemistry, Columbia University, New York.
25. Ferrin, T. E., Huang, C. C., Jarvis, L. E., and Langridge, R. (1988) *J. Mol. Graphics 6*, 13−27.
26. Kollman, P. A., Case, D., Singh, U. C., Alagona, G., Profeta, S., and Weiner, P. (1984) *J. Am. Chem. Soc. 106*, 765.
27. National Committee for Clinical Laboratory Standards (1997) *Methods for dilution antimicrobial susceptibility test for bacteria that grow aerobically*, 4th ed., approved standard M7-A4, National Committee for Clinical Laboratory Standards, Wayne, PA.
28. Link, A. J., Phillips, D., and Church, G. M. (1997) *J. Bacteriol. 179*, 6228−6237.
29. Metcalf, W. W., Jiang, W., Daniels, L. L., Kim, S. K., Haldimann, A., and Wanner, B. L. (1996) *Plasmid 35*, 1.
30. Gordon, J. J., Delvin, T. P., East, A. J., Ollis, W. D., Sutherland, I. O., Wrisly, D. E., and Ninet, L. (1975) *J. Chem. Soc., Perkin Trans. 1*, 819.
31. Attwood, M. M. (1969) *J. Gen. Microbiol. 55*, 209−216.
32. Huang, K., Shuji, T., Kinouchi, T., Takeyama, M., Ishida, T., Hisao, U., Datsuji, N., and Iwao, O. (1997) *J. Biochem. (Tokyo) 122*, 779−787.
33. Xu, Y., Lai, L., Gabrilove, J. L., and Scheinberg, D. A. (1998) *Clin. Cancer Res. 4*, 171−176.
34. Young, D., Rafanan, N., White, R., and Trias, J. (1999) *J. Bacteriol.* (submitted for publication).
35. Trias, J., and Gordon, E. M. (1997) *Curr. Opin. Biotechnol. 8* (6), 757−762.
36. Hu, Y., Wei, W., Zhou, Y., Rajagopalan, P. T. R., and Pei, D. (1999) *Biochemistry 38*, 643−650.
37. Ragusa, S., Mouchet, P., Lazennec, C., Dive, V., and Meinnel, T. J. (1999) *J. Mol. Biol. 289*, 1445−1457.
38. Rasmussen, H., and McCann, P. P. (1997) *Pharmacol. Ther. 75*, 69−75.
39. Whittaker, M., and Brown, P. (1998) *Drug Discovery Dev. 1*, 157−164.
40. Toba, S., Damodaran, K. V., and Merz, K. M. (1999) *J. Med. Chem. 42*, 1225−1234.
41. Broughton, B. J., Chaplen, P., Freeman, W. A., Warren, P. J., Wooldridge, K. R., and Wright, D. E. (1975) *J. Chem. Soc., Perkin Trans. 1 9*, 857−860.
42. Yamamoto, M., Tsujishita, H., Hori, N., Ohishi, Y., Inoue, S., Ikeda, S., and Okada, Y. (1998) *J. Med. Chem. 41*, 1209−1217.

BI992245Y